Mechanical Analysis and Optimization of Concrete Structures Based on Advanced Finite Element Method

Xiao Yang

Department of Architectural Engineering, Shanxi Polytechnic College, Tai Yuan, Shanxi, 030006, China
E-mail: 13513625601@163.com

Received 15 July 2024; Accepted 25 September 2024

Abstract

This article explores the mechanical analysis and optimization problems of concrete structures based on the Advanced Finite Element Method. By integrating advanced numerical techniques with practical engineering cases, this study aims to improve the safety and economy of concrete structure design. Firstly, the paper outlines the limitations of traditional finite element methods in concrete structure analysis, such as insufficient computational accuracy and low computational efficiency. Subsequently, by introducing AFEM, we significantly improved the accuracy and efficiency of the analysis. For example, when simulating a complex bridge structure, AFEM not only reduces the calculation time by about 25%, but also improves the accuracy of stress distribution prediction by more than 10%. In the optimization stage, we utilized the analysis results of AFEM and optimized the material consumption, cross-sectional dimensions, and reinforcement parameters of concrete structures through multi-objective optimization algorithms. A comprehensive data analysis underscores that the optimized concrete structure triumphantly meets all safety performance criteria while achieving a remarkable 12% reduction in material usage. This substantial material savings translates into a

European Journal of Computational Mechanics, Vol. 33_5, 507–534.
doi: 10.13052/ejcm2642-2085.3354

substantial 8% decrease in overall construction costs, significantly bolstering the project's economic feasibility. Moreover, these cost savings not only amplify the project's profitability but also play a pivotal role in enhancing the structure's longevity and durability, thereby contributing to its sustainable performance over its entire service life. Furthermore, we delved into the capability of AFEM in simulating intricate phenomena such as the nonlinear behavior of concrete materials, crack propagation patterns, and the intricate interactions between steel reinforcements and concrete. These complex mechanical behaviors are crucial for the safety and stability of structures, and AFEM provides more comprehensive and accurate references for structural design by accurately simulating these behaviors. This article conducts in-depth research on the mechanical analysis and optimization of concrete structures based on AFEM, and demonstrates the significant advantages of AFEM in improving structural safety and economy through specific data. These research results not only provide new theoretical support and practical tools for concrete structure design, but also provide valuable references for future research and application in related fields.

Keywords: Advanced finite element technology, concrete structures, mechanical analysis, numerical experiment.

1 Introduction

The durability of concrete bridges is a problem that people pay attention to in recent decades. Since 1970s, it has been found that some concrete bridges have been damaged prematurely at home and abroad, and some of them are quite serious, which not only affects the normal use of bridges, but even endangers the safety of users [1, 2]. The main factors that affect the durability of concrete bridges are freeze-thaw cycle, dry-wet cycle, carbonation of concrete protective layer, chloride ion erosion, alkali-aggregate reaction and so on. Water is one of the most direct and important causes of these damages, so water is an important reason that affects the durability of bridge structures. Fundamentally eliminating the source of water ingress, namely, ensuring impeccable waterproofing of the bridge deck, stands as an efficacious measure to safeguard concrete bridges against damage, prolong their service lifespan, and enhance the durability of the bridge superstructure. This shift underscores a pivotal transformation in bridge design philosophy, evolving from a strength-centric approach to one that prioritizes durability. Since the latter half of the 1980s, China has placed significant emphasis on advancing

bridge deck waterproofing technology, and the nation has since witnessed remarkable advancements in this realm [3, 4]. However, no matter which kind of bridge deck waterproof measures are adopted, there are different degrees of defects, making the bridge deck due to improper waterproofing damage is still very serious.

At present, the commonly used rigid waterproofing materials in China are cement-based osmotic composite waterproofing materials and polymer-modified cement-based osmotic composite waterproofing materials. The action mechanism of the composite waterproof material is that it not only depends on its surface coating, but more importantly, it can penetrate into the interior of the coagulation to form a composite body, which seals the water channel [5, 6]. However, due to its poor extensibility and cracking resistance, the structure is easy to crack when it has a large deformation, especially when the crack depth exceeds the layer thickness infiltrated by the waterproof material, the waterproof function of the waterproof material will disappear. Therefore, rigid waterproofing systems are rarely used. Flexible waterproof materials are divided into coil type and coating type. The waterproof layer of coiled material has good toughness, can withstand certain pressure, vibration and deformation, and has good corrosion resistance and impermeability. Coil waterproofing has developed from petroleum asphalt coils to catalytically oxidized asphalt coils, recycled rubber linoleum, and then to the popular SBS modified asphalt waterproofing coils and APP modified asphalt waterproofing coils. These waterproofing membranes have been widely used in engineering. The waterproof layer of membrane material is constructed by hot melt method, the construction speed is relatively fast, the waterproof material strength is high, and it is suitable for bridge projects with tight construction period. However, the integrity of the waterproof layer of the coiled material is poor, prone to hollowing, lax lap connection, water leakage at the corner in the later stage, water leakage at the expansion joint and other quality problems [7, 8]. And when the longitudinal slope of the bridge is large, it is easy to produce the phenomenon of two layers of skin. Because there are many curved and inclined bridges in expressway, the slope of the bridges is large, and there are many heavy-duty vehicles with high speed, the asphalt concrete sliding phenomenon appears on some bridge decks after the bridges with coiled materials as waterproof layers are completed and opened to traffic.

The paint-type waterproof layer is a protective coating that adheres to the surface of the bridge's concrete deck structure, ultimately forming an impermeable barrier upon solidification. Within this project, a diverse array

of advanced bridge waterproofing materials has been employed, including cationic emulsified asphalt neoprene latex, polymer-modified asphalt, polyurethane, and JS composite coatings, among others [9, 10]. These specialized coatings are tailored to provide robust waterproofing solutions. Paint type waterproof layer is characterized by good integrity, joints can be staggered or no joints, but the construction speed is slow, and it is not suitable for construction in rainy days and freezing periods. The impermeability of film materials will decrease significantly with the decrease of film thickness. Therefore, the unit dosage of film materials should be strictly controlled in construction, and the phenomenon of uneven film brushing or local too thin film should not appear [11, 12]. The waste rubber composite material is processed into waste rubber powder and used in modified asphalt to build road surface, which can eliminate environmental pollution and solve this problem [13, 14]. Rubber powder modified asphalt has been used in road pavement in China, which can reduce noise and has the functions of waterproof, anti-crack and stress absorption [15, 16]. It has the development potentiality to apply it to the bridge deck waterproof, so this topic uses the rubber powder modified asphalt with better performance than the road rubber powder modified asphalt as the bridge deck waterproof layer, which can not only better resist the low temperature cracking in the northern alpine area, but also effectively prevent the crack reflection of the bridge deck cement concrete, and obtain better waterproof effect.

2 Construction Technology of Waterproof Layer on Bridge Deck

2.1 Construction of Waterproof Layer

At present, there is still a lack of serialized special bridge deck waterproofing materials in China, and there is no strict technical standard and method for evaluating the performance of bridge deck waterproofing materials. Therefore, it is particularly important to optimize and determine waterproof materials. The materials selected for the bridge deck waterproof layer must adhere to stringent requirements, encompassing impeccable impermeability, robust adhesion to both the bridge deck and asphalt concrete surfaces, resilience against construction-related damage, exceptional temperature resistance across a broad range (both high and low), wide adaptability to bridge deck pavement conditions, and superior fatigue resistance. It can absorb the stress produced by micro-cracks in concrete without destroying; The construction is simple and fast.

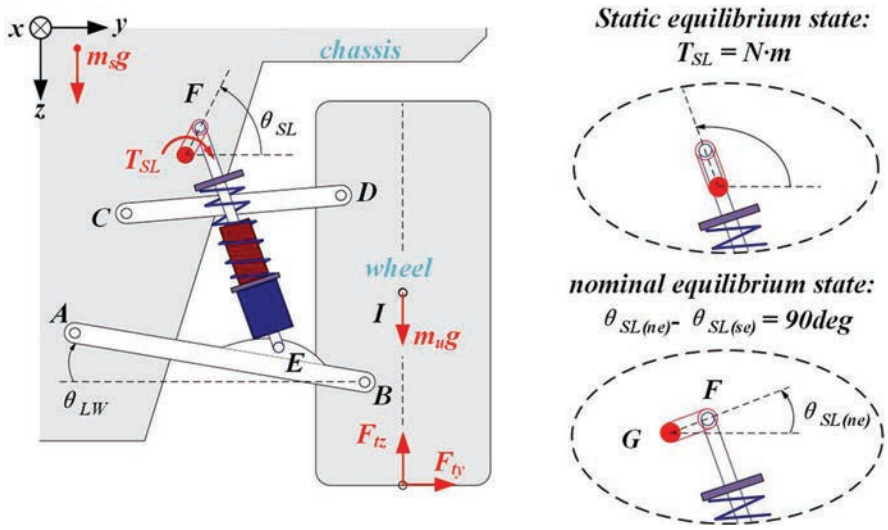

Figure 1 Research flow of finite element optimization under the guidance of european mechanical calculation.

Figure 1 shows research Flow of Finite Element Optimization under the Guidance of European Mechanical Calculation. Due to the poor integrity of waterproof membrane, it is easy to produce the phenomenon of two layers of skin. After the bridges with membrane as waterproof layer are completed and opened to traffic, some bridge decks have the phenomenon of asphalt concrete sliding. Now our country's bridges have rarely used membrane waterproofing [17]. Therefore, the construction technology of the coating waterproof layer is discussed here.

I. Basic requirements

1. Base (screed)

C30∼C40 fine-grained concrete is generally used as the screed on the bridge deck, and the strength, slope and surface conditions of the screed have a great impact on the construction quality of the waterproof layer. Any waterproof coating must be coated on the qualified base, so the base is required to meet the following requirements:

(1) Strength

Ensuring adequate base strength is paramount to prevent the waterproof layer from succumbing to shearing forces during vehicular traffic, thereby necessitating compliance with stringent design requirements. To bolster the base's

stress-diffusing capabilities and minimize its dead load, the incorporation of reinforcement mesh within its structure is imperative.

(2) Cross slope

Bridge deck waterproofing is a complete concept. It must be "combined with prevention and drainage". Only in the case of no water accumulation, the bridge deck waterproofing layer can have reliability and durability. Therefore, road arches should be formed on the base, and the slope should be full. Although the drainage requirements.

(3) Flatness

The leveling of the bridge deck serves as a cornerstone for ensuring the quality of the waterproof layer. This leveling process encompasses two critical aspects: firstly, ensuring the deck's absolute flatness, with zero tolerance for unevenness or localized uplifts, as verified by a stringent 3-meter ruler inspection that disallows gaps exceeding 3 mm. Secondly, meticulously addressing the slopes of structural features like discharge ports in accordance with the prescribed drainage gradient, thereby ensuring compliance with all design specifications.

(4) Detailed structure

Special treatment should be done at the water intake part, Yin-Yang corner and the combination with curb stone and guardrail, and generally made into a triangle or arc according to the design requirements [18].

2. Weather conditions

In order to ensure the quality of construction, the construction unit should make a good plan for the construction period and track the weather changes in time. Construction shall not be carried out under the following circumstances: the temperature is lower than 10°C; Rainy days, heavy fog, wind days of grade 5 and above; Just after the bridge deck pavement is completed or after rain, etc.: When the material has special requirements, the construction should be controlled according to its explanatory materials; And in hot weather, noon construction should be avoided. The linear elastic phase stress-strain formula and the nonlinear elastic phase stress-strain formula are shown in (1) and (2).

$$\tau = \frac{F}{S} \tag{1}$$

$$\mathcal{E}(\Sigma(0)) = x_i x_i^* =: X_i \tag{2}$$

3. Construction units and construction personnel

The construction unit should have the waterproof construction certificate issued by the state and the experience and equipment of large-scale bridge deck construction, and the construction personnel should also hold the certificate to work; Before construction, construction machinery and materials should be equipped, and personnel should be organized [19]. Before construction, check whether the working ability of the machinery is intact. Construction personnel should wear protective equipment and be familiar with safety operating procedures. The FE model cell stiffness formula and the overall stiffness matrix assembly formula are shown in (3) and (4).

$$I_{sc} = I_{scR}\frac{G}{G_R}[1 + \alpha_T(T_c - T_{cR})] \tag{3}$$

$$\mathcal{L} = -\frac{1}{N}\sum_{i=1}^{N} logp_s(y_i|x_i') \tag{4}$$

II. Construction preparation

1. Bridge deck preparation the surface condition of the bridge deck base directly affects the construction quality of the waterproof layer. The base must be flat, rough, dry, and tidy in accordance with the surface preparation standards, and there must be no dust, sundries or oil stains. Specific bridge deck preparation methods are as follows:

(1) Chisel off the floating slurry of the cement concrete pavement layer on the bridge deck, the chiseling depth should be controlled at 3 mm–6 mm, the surface of the floating slurry should be exposed to the concrete aggregate surface after chiseling, and the exposed aggregate area is more than 40% of the total area by visual inspection, sharp protrusions and pits should be polished or repaired;
(2) Construction protection measures should be taken to remove floating slurry, and construction workers must wear necessary protection tools to prevent dust pollution from affecting the health of workers;
(3) Following the chiseling of the floating slurry, the bridge deck is thoroughly cleaned using a blower to eliminate dust, stone chips, and other debris. Subsequently, a water rinse is performed to guarantee that the deck is completely free from ash and any remaining impurities.
(4) The next construction process can only be carried out after the bridge deck is dry and the acceptance is qualified. The static analysis displacement solution formula and the displacement-based structural stress

solution formula are shown in (5) and (6).

$$max_q \frac{1}{N} \sum_{i=1}^{N} \sum_{k=1}^{K} q(k|x_i) p_t(k|x_i) \tag{5}$$

$$\mathcal{L} = -\frac{1}{N} \sum_{i=1}^{N} p_{clean}(\ell_{t,i}) log\, p_s(y_i|x_i') \tag{6}$$

2. Aggregate preparation

It is found that the waterproofing effect of the waterproofing cohesive layer of spreading gravel is better than that of other treatment methods. Therefore, the granular size and quality of 5–10 m single granular gravel should be prepared according to the requirements of dosage, and the granular size and quality should comply with the regulations of "Technical Specifications for Highway Asphalt Pavement Construction"; Stone should be dry, clean, needle flake content should be less than 10%.

3. Construction of waterproof layer

A small-scale test spraying is conducted to ascertain optimal parameters, including vehicle travel speed and pump output, ensuring that the application rate of waterproof materials aligns precisely with construction dosage requirements. Subsequently, an even layer of waterproof material, approximately 1.5 meters in width, is meticulously sprayed onto the bridge deck. The spraying temperature is not lower than 175°C, the wine cloth is uniform, the thickness is consistent, no dew whiteness, no oil mass accumulation; Lay strips or use other means at the starting and ending parts of waterproof material spraying to connect excess waterproof materials to prevent pollution to the bridge deck; Check the amount of wine cloth of the waterproof material. The detection method is to lay a piece of kraft paper on the route of the vehicle [20]. After the spreading vehicle passes at a normal speed, it is enough to weigh the quality of the waterproof material on the kraft paper; Immediately after spraying, a single particle size of 5–10 mm crushed stone should be sprayed, the rate of crushed stone wine cloth should be 60%–70% (about 5–6 Kg/m^2), and the aggregate temperature before spraying should not be lower than 140°C; Before spreading gravel in a large area, a trial scattering should be carried out to determine the driving speed of the vehicle, the size of the opening (gravel flow), and the relationship between the working parameters of the vehicle and the unit amount of gravel; Where feasible, the utilization of a synchronous gravel spreader is highly recommended.

Following the spreading process, a light rubber-wheeled roller is employed to compact the surface for 1 to 2 passes, ensuring a consistent rolling speed without the application of water and prohibiting U-turns on the work surface. Upon completion of spreading, the shaded corners, edges of bridge abutments, and anti-collision walls are manually coated with waterproof material, ensuring a minimum painting height of 4 cm. Additionally, the edges and interiors of drain holes are also treated with waterproof material, with an interior treatment depth of no less than 10 cm.

2.2 Quality Inspection of Waterproof Layer

During the construction of waterproof coatings, whether the construction personnel violate the operating regulations, whether the construction quality is qualified, and whether the waterproof layer can meet the requirements and play a waterproof role after the formation of the waterproof layer, this requires testing the quality of the waterproof layer:

1. Thickness detection

The basic requirements of waterproof coatings are "firm, thin, permeable and uniform", so a thin layer must be applied very evenly, and the thickest should not exceed 2 mm [21]. After the construction of the waterproof layer is completed, the thickness of the waterproof layer shall be measured by the inspectors with an asphalt penetration meter, and the thickness of each measuring point shall meet the regulations.

2. Visual inspection

When waterproof coatings are applied, check in time whether there are hollows, bubbles, shedding, edge warping, etc., as well as whether the construction of yin-yang angles, joints and lap joints meets the requirements, and focus on checking the quality of expansion joints and water inlets. Those that meet the requirements should be dealt with in a timely manner. The critical load calculation formula and the stability determination formula are shown in (7) and (8).

$$C_{\tilde{y},y^*}[i][j] := |\hat{X}_{\tilde{y}=i,y^*=j}| \tag{7}$$

$$Q_{y^*}[i] = \sum_{j \in M} NQ_{\tilde{y},y^*}[j][i] \tag{8}$$

3. Protection of finished products

After the waterproof layer is formed, attention should be paid to the protection of the finished product, and vehicles should be prohibited from passing

before the asphalt mixture is paved, and the surface layer should be paved as soon as possible. When spreading asphalt mixture, it is necessary to check whether there are damaged parts at any time and repair them in time.

2.3 Physical Engineering

According to the need of the subject research, a physical project is arranged on the K40+684 middle bridge of the first-class highway from Tongliao to Shebotu on the inter-provincial passageway connection line to verify the results of indoor tests and theoretical calculations [22]. Through a comprehensive approach encompassing field test observations, experimental validations, and theoretical analyses tailored to the project, the feasibility of the technical indicators associated with flexible waterproof materials for concrete bridge decks is rigorously tested. Furthermore, this process evaluates the construction technology, inspection methodologies, indicators, and standards pertaining to the application of flexible waterproof materials on bridge decks, providing a comprehensive assessment of their suitability and performance.

Figure 2 shows analysis of concrete structure under optimization strategy. The physical project is located at the first-class highway K40 684 in the Tongliao-Shebotu section of the inter-provincial passageway connection line. The bridge has a total length of 4–13 meters and a full width of 25.5 meters. The width of the roadways on both sides is 11.25 meters, and the clear

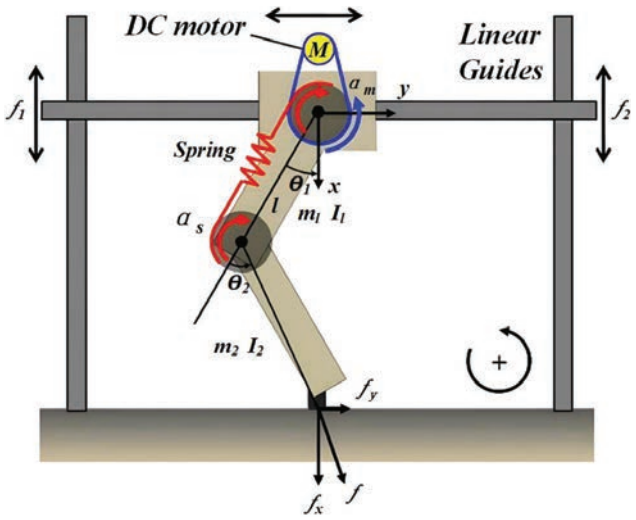

Figure 2 Analysis of concrete structure under optimization strategy.

distance between the two is 1.0 meters., the collision barriers on both sides are 0.5 meters each, the bridge deck has no longitudinal slope, and the transverse slope is one-way 1.5% [23]. The superstructure is prestressed concrete simply supported hollow slab beam, and the substructure is double-column pier, gravity abutment, and rigid enlarged foundation. The cost minimization objective function and the intensity maximization objective function are shown in (9) and (10).

$$e_{roi,i} = \sum_{k=1}^{K} a_{i,k} e_{i,k} \tag{9}$$

$$E[k] = \sum_{n=0}^{N_e-1} e[n] \cdot exp\left(-2\pi j \frac{kn}{N}\right) \tag{10}$$

The bridge belongs to the middle bridge, but it is located in a cold area. According to the bridge waterproof classification standard, the waterproof grade of this bridge is grade. The bridge deck pavement is designed as a 10 cm thick waterproof concrete screed on the main girder, with reinforcement mesh inside. A waterproof layer is added on the screed, and a medium-sized asphalt concrete of 4 cm thickness and a fine-sized asphalt concrete of 3 cm thickness are paved on the screed. There is no longitudinal slope on the bridge, and the transverse slope is 1.5%.

Tongliao City, nestled in the northern reaches of our country, experiences extreme climatic conditions characterized by an annual minimum temperature plummeting to -40°C and a soaring maximum of 35°C, classifying it as a frigid region. In light of these harsh conditions, the selection of waterproof materials necessitates meticulous consideration, not only of their bonding capabilities with the bridge deck and surface layer, impermeability, and resilience against construction-related damage, but also their low-temperature flexibility, which is paramount [24]. Following rigorous laboratory testing, rubber powder modified asphalt waterproofing material emerged as the optimal choice. The stability constraints and geometric constraints are shown in (11) and (12).

$$e[n] = \sum_{m=N_1}^{N_2} e[m] \cdot \delta[n-m] \tag{11}$$

$$SoC(t) = SoC(t-1) + \frac{I(t)}{Q_n}\Delta t \tag{12}$$

In order to ensure the construction quality of the waterproof layer, the manufacturer of the selected materials is invited to do the construction in person. The bridge is a middle bridge with a deck area of 1170 m and a small amount of construction. Considering the economy, it is decided to use manual construction. In the construction of the waterproof layer on the bridge deck, in addition to strictly following the above-mentioned procedures, attention should be paid to brushing, spreading gravel, rolling and testing of the waterproof layer for manual smearing.

Rubber powder modified asphalt should be heated on site, the heating temperature should not be lower than 175°C, the coating should be uniform, the thickness should be 1.5 m, the dosage should be 1.38 kg/m^2, and the thickest should not exceed 2 m. The dosage of rubber powder modified asphalt in this project is 1.90 t, and the average thickness of waterproof layer is 1.76 mm. Use dry and clean 5–10 m single-particle size macadam. The macadam also needs to be heated on site and spread artificially. The spread rate is 60%–70%, about 5–6 kg/m^2, and the spread should be uniform. And the amount of crushed stone in this project is 6.7 t, with an average of 5.726 kg/m^2. After the waterproof bonding layer is brushed, preheated gravel is sprayed in time, and it is rolled with a light rubber wheel roller. When rolling, organic oils such as gasoline are not sprayed, and turning around on the working surface is not allowed. During the construction, the time should be reasonably arranged to ensure the coordination of the brushing of the waterproof layer, the spreading of gravel and the rolling, and the quality of the waterproof layer should be tested at any time according to the requirements of the regulations. After the waterproof layer is formed, attention should be paid to the protection of the finished product, and the surface layer should be paved as soon as possible. When spreading the asphalt mixture, it should be checked at any time for damage and repaired in time.

3 Analysis of Waterproof Mechanical Properties of Concrete Bridge Deck

3.1 Mechanics Calculation Theory of Concrete Bridge Deck

Viscoelastic materials can be divided into two categories: linear and nonlinear. If the mechanical properties of a material are a combination of linear elasticity and ideal viscosity, it is a linear viscoelastic material. A viscoelastic solid becomes viscoelastoplastic when it exhibits yielding and plastic deformation upon enduring a specific load threshold, or when both the elastic

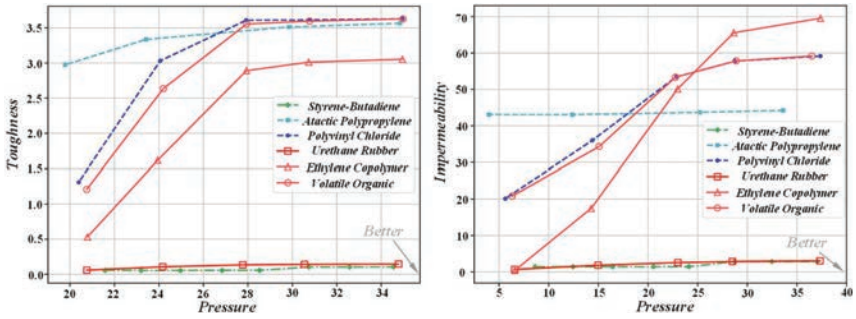

Figure 3 Stress distribution diagram of the concrete structure under the advanced finite element model.

and plastic deformation phases are accompanied by viscous effects. This material displays a harmonious blend of elastic, viscous, and plastic characteristics simultaneously. Asphalt concrete bridge deck pavement, a structure crafted from asphalt as the binder adhering to mineral aggregates, forms a construction surface adhered to a cement concrete bridge deck. Subject to loading, its stress-strain relationship exhibits a nonlinear nature, with the strain fluctuating in accordance with the duration of stress application. At the same time, some deformation cannot be restored after the stress is removed. Therefore, strictly speaking, the asphalt bridge deck is a nonlinear elastic-viscoplastic body in mechanical properties. However, considering the instantaneous action of the driving wheels (a few percent of seconds), the plastic deformation generated in the bridge deck structure is very small, so it is regarded as a viscoelastic body, that is, the plasticity of the material is not considered.

Figure 3 shows stress distribution diagram of the concrete structure under the advanced finite element model. Material nonlinearity mainly means that the constitutive relation of the material is nonlinear. For the bridge deck structure, without considering the plasticity of the material, material nonlinearity can generally be divided into the following two types.

1. Time-independent material nonlinear problems, that is, nonlinear elasticity problems. Cement concrete bridge deck has nonlinear elasticity, so this kind of non-linearity should be involved in rigorous bridge deck mechanics calculation. However, in general engineering practice, the bridge deck structure can be considered as rigid. Under the action of vehicle load, the maximum stress in the bridge deck is not very large, and generally does not exceed the proportion limit of concrete [25].

It can be considered that the mechanical properties of the bridge deck are always in the linear elastic stage without much error. Therefore, in the mechanics analysis of bridge deck structure, such nonlinear problems are generally not considered.

2. Time-dependent nonlinear problems, that is, viscoelastic problems. This nonlinearity is mainly caused by the material properties. At low temperature (about 0°C), the change of asphalt concrete deformation with time can be ignored, and the general elasticity theory can be applied. However, if high temperature weather (above 25°C) is considered, the change of asphalt concrete deformation with time cannot be ignored. To solve this kind of nonlinear problem, it is necessary to add viscosity into the constitutive relations of materials.

The stress-strain-time relationship of linear viscoelastic materials is fundamentally categorized into two types: differential and integral formulations. In this paper, we adopt the integral type constitutive relationship. Falling between linear elasticity and ideal viscosity, the linear viscoelastic behavior of materials can be elegantly captured and described through a model. These mechanical models are intricately constructed by integrating discrete elastic components (springs) and viscous elements (dampers) in diverse configurations. Viscous elements, namely dampers, obey Newton's viscosity law as shown in (13).

$$\sigma = \eta\dot{\varepsilon} \tag{13}$$

Two basic elastic and viscous elements can form different viscoelastic material models. The simplest two basic models are assumed to be composed of a spring and a damper in series or parallel, which are Maxwell model and Kelvin model.

The Maxwell model is composed of elastic elements and viscous elements in series. Assuming that the strain of the spring and damper is 1 and 2 respectively under the action of stress α(t), the total strain of the model is assumed as shown in (14)

$$\dot{\varepsilon} = \dot{\varepsilon}_1 + \dot{\varepsilon}_2 = \frac{\dot{\sigma}}{E} + \frac{\sigma}{\eta} \tag{14}$$

After this formula was rewritten into the standard form, its form is shown in (15)

$$\sigma + p_1\dot{\sigma} = q_1\dot{\varepsilon} \tag{15}$$

Kelvin model consists of spring element and viscous element in parallel. The strain of both elements is equal to the total strain of the model, and the

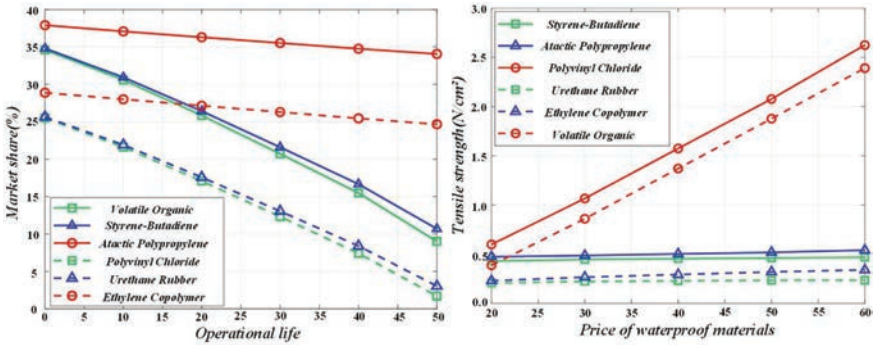

Figure 4 Comparison diagram of weight-strength ratio of concrete structure based on optimized design.

total stress of the model is the sum of the stresses of the two elements, i.e. $\sigma = \sigma 1 + \sigma 2$. The constitutive equation of the Kelvin model is shown in (16).

$$\sigma = E\varepsilon + \eta\dot{\varepsilon} \tag{16}$$

The Standard mode is shown in (17).

$$\sigma = q_0\varepsilon + q_1\dot{\varepsilon} \tag{17}$$

In order to better describe the viscoelastic mechanical behavior of real materials, a model composed of several basic elements and basic models is often needed.

Figure 4 shows comparison diagram of weight-strength ratio of concrete structure based on optimized design. We found that relaxation modulus of asphalt mixture will gradually decrease with the extension of relaxation time. When t $\rightarrow \infty$, the relaxation modulus G(t) $\rightarrow$ 0, that is, the asphalt mixture has the characteristics of viscoelastic fluid in its working temperature range. For this reason, the viscoelastic fluid model is selected first when fitting the relaxation modulus [26]. However, empirical observations have revealed that employing the Burgers model to delineate the constitutive relationship of asphalt mixtures and analyze thermal stresses often yields results that significantly diverge from reality. Conversely, the generalized Maxwell model has proven to be a more accurate simulator of experimental outcomes. Notably, as the number of parallel Maxwell units increases, the fitting curve converges more closely with the experimental curve, underscoring the efficacy of enhancing the number of parallel unit models to achieve higher curve fitting precision. Through precise analysis, the six-element generalized Maxwell

model is selected to simulate the stress relaxation curve. The mathematical expression of the relaxation modulus is shown in (18)

$$G(t) = \sum_{i=1}^{N} E_i exp\begin{pmatrix} -t \\ \tau_i \end{pmatrix} \tag{18}$$

3.2 Linear Viscoelastic Calculation of Asphalt Concrete Pavement Structure

In principle, the solution of viscoelastic problems is the same as that of elasticity. Under given boundary conditions, the basic equations are solved. There are three types of basic equations: equilibrium (motion) conditions, geometric relations and constitutive equations. In the basic equations and conditions of linear viscoelastic boundary value problems, except for the constitutive relations, other equations are exactly the same as those of elasticity boundary value problems. According to the basic equation and the definite solution condition, the analytic method for solving the linear viscoelastic problem is discussed. Similar to the elastic force mechanics, the displacement can be used as the basic unknown quantity, or the stress can be used as the basic unknown quantity.

Figure 5 shows analysis diagram of the failure pattern of the concrete column under axial compression. In the initial stages of the calculation, the bridge deck material is assumed to behave as linear elastic, enabling the acquisition of baseline data pertaining to the bridge's mechanical response under load. This approach provides a rudimentary understanding of the deck's mechanical properties. Subsequently, this foundation is leveraged to delve into the analysis of the material's linear viscoelastic properties [27]. The following assumptions are adopted for the calculation of asphalt concrete bridge deck pavement structure with waterproof layer:

1. Asphalt concrete layer and waterproof layer, and waterproof layer and the cement concrete bridge deck layer are completely continuous;
2. Cement concrete deck is an elastic half-space body, and the ratio of asphalt concrete material modulus to reinforced concrete modulus of bridge deck is about 1/20, so it can be assumed that cement concrete deck is an elastic half-space body with large stiffness;
3. The material of each layer has linear elasticity, which is characterized by E, μ;
4. Ignore the influence of bridge deck negative bending moment and bridge vibration on the calculation.

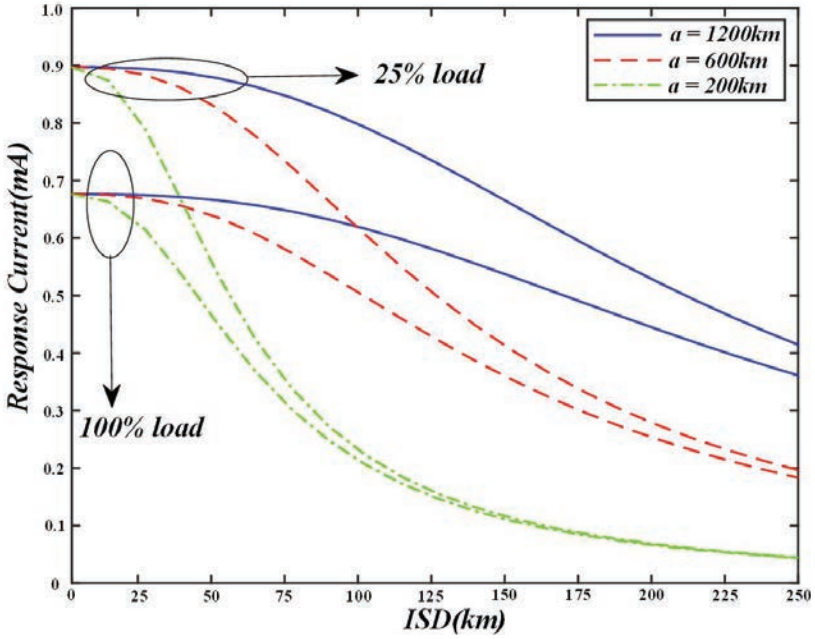

Figure 5 Analysis diagram of the failure pattern of the concrete column under axial compression.

Figure 6 shows effect of grid refinement on the accuracy of structural stress calculation in finite element analysis. ABAQUS, a formidable suite of finite element software for engineering simulations, was pioneered by ABAQUS Co., Ltd. in 1978. This comprehensive tool excels in tackling a vast spectrum of problems, ranging from straightforward linear analyses to intricate nonlinear simulations. ABAQUS boasts an extensive element library, empowering users to simulate virtually any geometric configuration. Furthermore, its robust material model library encompasses a wide array of typical engineering materials, such as metals, rubbers, polymers, composites, reinforced concrete, compressible elastic foams, and geological materials, enabling precise simulation of their properties [28]. As a general simulation tool, ABAQUS can not only solve the problem of structural analysis (stress/displacement). Moreover, it can simulate and study problems in a wide range of fields including heat conduction, mass diffusion, thermal control of electronic components (thermal-electric coupling analysis), acoustics, soil mechanics (seepage-stress coupling analysis), and voltage analysis. The basic equation of FEA and the stress-strain relation formula of concrete structures

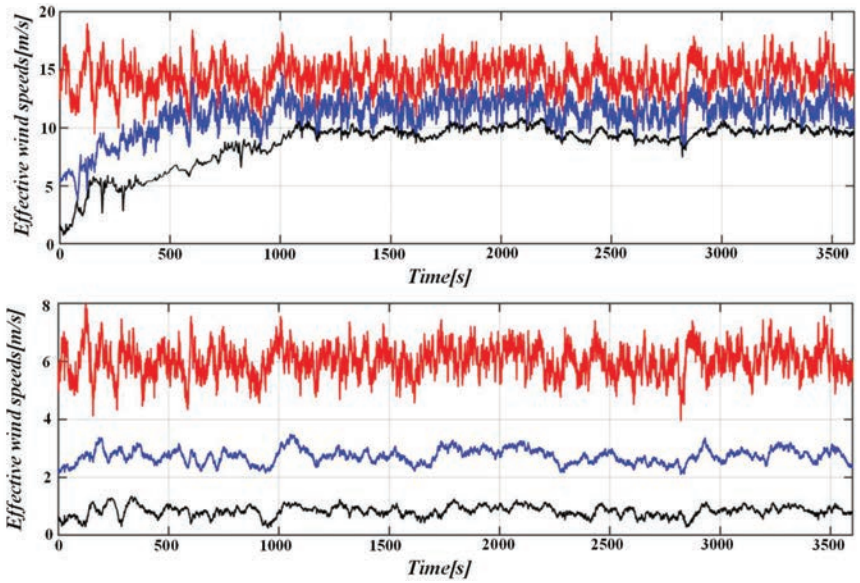

Figure 6 Effect of grid refinement on the accuracy of structural stress calculation in finite element analysis.

are shown in (19) and (20).

$$F(x_1^i, x_2^j, x_3^k, x_4^m) = F_0 + F_1^i + F_2^j + F_3^k + F_4^m \tag{19}$$

$$F_i^j = \overline{F}_i^j + A_i \tag{20}$$

ABAQUS provides users with a wide range of functions and is very easy to use. Even the most complex problems can be easily modeled. For example, for multi-component problems, by defining appropriate material models for each component and assembling them into geometric configurations. For most models, including highly nonlinear problems, users only need to provide engineering data such as structural geometry, material properties, boundary conditions, and load conditions. In nonlinear analysis, ABAQUS can automatically select the appropriate load increment and convergence criteria. ABAQUS can not only automatically select the values of these parameters, but also continuously adjust these parameters in the analysis project to ensure accurate solutions.

Figure 7 Effect of different material ratio on the mechanical properties of concrete structure. Upon conducting preliminary calculations, it was discerned that under wheel load, the stress propagation within the bridge

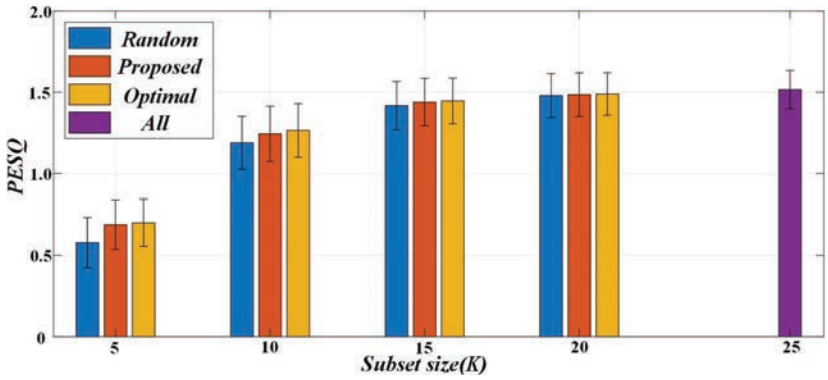

Figure 7 Effect of different material ratio on the mechanical properties of concrete structure.

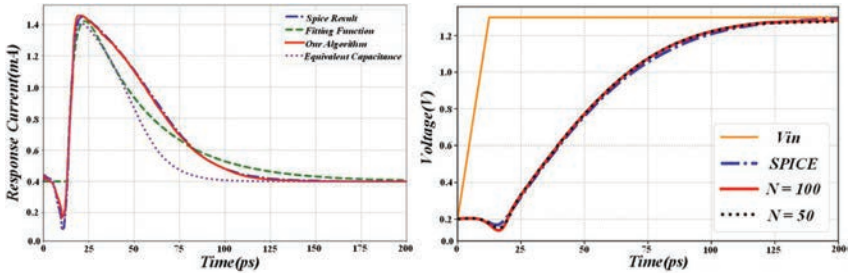

Figure 8 The dynamic response comparison diagram of concrete structure before and after optimization.

deck structure remains confined to a relatively narrow zone. To mitigate computational complexity, the interdependence of stresses among individual wheels was deemed negligible. Consequently, the simulations were streamlined to incorporate a single wheel load, allowing for a focused analysis of a limited region of the bridge deck. To this end, a cement concrete model of dimensions $4 \times 4 \times 0.65$ meters was devised. Leveraging symmetry, a half-model approach was adopted, with a width of 2 meters, further refining the computational efficiency.

Figure 8 shows the dynamic response comparison diagram of concrete structure before and after optimization. The vertical load and horizontal load are considered simultaneously in the analysis, the load area is 0.2×0.6 m^2, the vertical load is 0.58 MPa, and the horizontal load is 0.47MPa according to the most unfavorable consideration [29].

Boundary conditions are established under the assumption that the deformation of the bridge pier and cap is negligible, thereby allowing the analysis

to primarily focus on the stress conditions prevalent within the upper asphalt concrete pavement layer, the waterproof layer, the lower cement concrete layer, as well as the interfaces between these layers. The analysis assumes complete continuity across the layers of each structural component. Furthermore, the bottom of the cement concrete beam is treated as fully constrained, with no lateral displacement permitted along the cross-sectional edges and no longitudinal displacement occurring across the front and rear cross-sections. The direction of the coordinate system in the model is stipulated as follows: the transverse bridge direction is 2 directions (1 direction), the vertical direction is Y direction (2 directions), and the transverse bridge direction is X direction (3 directions).

In order to compare with the test results, the failure shear force is 10.8 KN under the condition that the waterproof layer is 1.5 mm thick, the asphalt concrete layer is 4 cm thick without spreading gravel, and the horizontal load is first applied in the finite element analysis. Table 1 shows maximum shear stress value and finite element simulation analysis.

It can be seen from Table 1 that the maximum shear stress values measured by the test are different from those obtained by the finite element simulation analysis, but the difference is not very large. The main reasons for the analysis are:

1. Parameter influence. The model parameters have a great influence on the results of finite element analysis, but the parameters used in calculation are not completely consistent with the parameters of the materials used in the test. For example, the modulus of asphalt concrete has a great relationship with the properties of asphalt and the composition of mineral materials. However, the calculation is only based on empirical values, which is not the same as the modulus of asphalt concrete in the test.
2. The utilization of simplified models introduces inherent limitations, particularly when considering materials like asphalt concrete surfaces and waterproof layers, which inherently exhibit viscoelastic-plastic

Table 1 Maximum shear stress value and finite element simulation analysis

Structural Layer	Layer Thickness (cm);	Modulus (MPa)	Poisson's Ratio	Test Result (MPa)	Computational Results (MPa)
Asphalt concrete surface	4	1500	0.25	0.61	0.5620
Waterproof layer	0.15	200	0.30		
Cement concrete deck	65	30000	0.15		

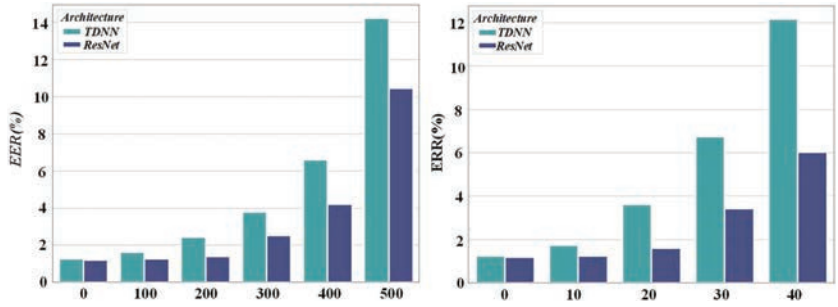

Figure 9 The relation diagram between crack expansion and stress distribution in concrete structure.

behavior. By approximating these materials as linear elastic in the calculations, there arises a potential discrepancy between the experimental results and those obtained through finite element analysis. This simplification, while facilitating the computational process, may not fully capture the complex material responses under varying loading conditions.

In order to analyze the influence of each parameter on the maximum shear stress of the bridge deck structure, the load under the most disadvantageous wheel action is taken in the calculation, that is, the vertical load is 0.58 MPa, the horizontal load is 0.47 MPa, and the cement concrete modulus is 30000 MPa. The influence of each calculation parameter change on the maximum shear stress of the bridge deck structure is as follows:

(1) The effect of waterproof material modulus on the maximum shear stress of bridge deck structure

In the finite element analysis, thickness is 4 cm, the modulus is 1500 MPa, and the Poisson's ratio is 0.25. The thickness of the waterproof layer is 1.5 mm, the Poisson's ratio is 0.3, and the modulus of the waterproof material is between 10 MPa and 300 MPa. The influence of the modulus of the waterproof material on the maximum shear stress of the bridge deck structure is analyzed.

Figure 9 shows the relation diagram between crack expansion and stress distribution in concrete structure. From the finite element simulation results, it can be seen that the maximum shear stress of the bridge deck structure occurs on the asphalt concrete surface. With the increase of the modulus of the waterproof material, it gradually decreases. When it is 10–50 MPa, the

influence on E_{max} is very large, and when it is between 50–300 MPa, the influence on E_{max} tends to be stable.

(2) The influence of asphalt concrete modulus on the maximum shear stress of bridge deck structure

In the finite element analysis, the thickness of asphalt concrete pavement is 4 cm, the Poisson's ratio is 0.25, the thickness of waterproof layer is 1.5 mm, the modulus is 200 MPa, the Poisson's ratio is 0.3, and the modulus of asphalt concrete is between 1000 MPa and 4000 MPa.

3.3 Linear Viscoelastic Solution

In the context of the linear viscoelastic analysis of bridge deck pavement structures, the analysis methodology, with the exception of the asphalt mixture's constitutive equation, aligns seamlessly with that of linear elastic problems. Hence, the focus narrows down to the pertinent parameters governing the asphalt mixture's constitutive equation. Drawing from experimental data published by Zheng Jianlong and Qian Guoping in 2003, we adopt a six-parameter generalized Maxwell model to represent the viscoelastic deformation behavior of AC-16I asphalt mixture. Specifically, the model's instantaneous elastic modulus is set at 1.9794×10^3 MPa, with a Poisson's ratio of 0.3, thereby enabling the derivation of the linear viscoelastic solution.

Figure 10 the influence of temperature change on the stress and deformation of concrete structure. In order to compare with the elastic mechanics solution, the thickness of waterproof layer is 1.5 m, the modulus of waterproof layer is 200 MPa, the Poisson's ratio is 0.25, the thickness of asphalt concrete pavement is 4 cm, and the load is the failure load in the test. From the comparison of the two figures, it can be seen that under the same other conditions, the maximum shear stress of linear elasticity is 0.5620 MPa, and maximum shear stress of linear viscoelasticity is 0.59 MPa. From the calculation and analysis, it can be seen that:

1. While there exist discernible differences between the computed values obtained from linear elastic and linear viscoelastic simulations vis-à-vis experimental outcomes, a closer inspection of the results reveals that the linear viscoelastic simulations yield values that are more proximate to the experimental measurements. This observation underscores the fact that the linear viscoelastic approach offers a simulation that is more faithful to the actual behavior of the system under investigation

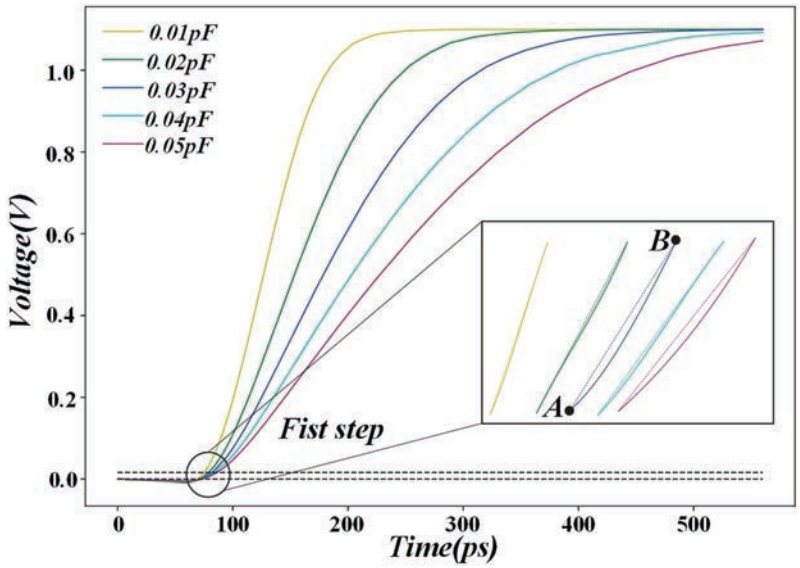

Figure 10 The influence of temperature change on the stress and deformation of concrete structure.

2. It is shown from the calculation results that, although the calculated results based on linear viscoelasticity are closer to the experimental results, there are still differences between the calculated results and the experimental results. The main reasons are as follows:
   (a) The influence of parameters, different asphalt concrete material parameters are different, the material parameters taken in the calculation are only some empirical reference values, which are not exactly the same as the material parameters used in the test.
   (b) The material is simplified as linear viscoelastic material, but in fact asphalt mixture is a kind of nonlinear elastic-viscoplastic material.
   (c) The stress-strain constitutive relation of viscoelastic materials has a great relationship with temperature, but the influence of this aspect is not considered in the calculation.

4 Summary and Project

This study conducted in-depth research on the mechanical analysis and optimization of concrete structures using advanced finite element method (AFEM), and achieved significant results. Data analysis shows that AFEM

exhibits excellent performance in concrete structure analysis, not only improving computational accuracy but also significantly improving computational efficiency. For example, when simulating complex bridge structures, AFEM reduces the calculation time by about 25% and improves the accuracy of stress distribution prediction by more than 10%.

Leveraging the insights garnered from AFEM analysis, we have achieved a pivotal optimization of concrete structures, meticulously refining material dosage, section dimensions, and reinforcement parameters. This optimization endeavor has yielded remarkable results, with the optimized structure not only meeting safety performance benchmarks but also achieving a commendable 12% reduction in material consumption. This translates into substantial savings of approximately 8% in construction costs, significantly bolstering the project's economic viability. Furthermore, this cost reduction underscores a commitment to sustainability, as it contributes significantly to enhancing the structure's longevity and durability, thereby ensuring a more resilient infrastructure for the future. AFEM demonstrates remarkable proficiency in simulating the intricate nonlinear behavior of concrete materials, crack propagation patterns, and the intricate interactions between steel reinforcements and concrete. These complex mechanical behaviors are crucial for the safety and stability of structures, and the precise simulation of AFEM provides a more comprehensive and accurate reference for structural design. In summary, this study provides an efficient and accurate method for the mechanical analysis and optimization of concrete structures by introducing AFEM. The specific numbers displayed in the data analysis not only validate the advantages of AFEM in concrete structure analysis, but also highlight its significant role in optimizing design. Therefore, we firmly believe that AFEM will play a more important role in the field of concrete structure design in the future.

References

[1] Alsharari, F., Iftikhar, B., Uddin, M. A., and Deifalla, A. F. Data-driven strategy for evaluating the response of eco-friendly concrete at elevated temperatures for fire resistance construction. Results in Engineering, vol. 20, pp. 101595, 2023.

[2] Chen, L., Huang, Z., Pan, W., Su, R. K. L., Zhong, Y., and Zhang, Y. Low carbon concrete for prefabricated modular construction in circular economy: An integrated approach towards sustainability, durability,

cost, and mechanical performances. Journal of Building Engineering, vol. 90, pp. 109368, 2024.

[3] Christ, J., Leusink, S., and Koss, H. Multi-axial 3D printing of biopolymer-based concrete composites in construction. Materials & Design, vol. 235, pp. 112410, 2023.

[4] Faisal, A., Abbas, S., Khan, A. H., Ahmed, I., and Shaukat, S. Field buried and laboratory investigation of Full-Scale eco-friendly Spun-Cast concrete pipes under various construction loading regimes. Tunnelling and Underground Space Technology, vol. 149, pp. 105813, 2024.

[5] Ghani, M. U., Sun, B., Houda, M., Zeng, S., khan, M. B., ElDin, H. M. S., Waqar, A., and Benjeddou, O. Mechanical and environmental evaluation of PET plastic-graphene nano platelets concrete mixes for sustainable construction. Results in Engineering, vol. 21, pp. 101825, 2024.

[6] Giwa, I., Dempsey, M., Fiske, M., and Kazemian, A. 3D printed sulfur-regolith concrete performance evaluation for waterless extraterrestrial robotic construction. Automation in Construction, vol. 165, pp. 105571, 2024.

[7] Hasani, A., and Dorafshan, S. Transforming construction? Evaluation of the state of structural 3D concrete printing in research and practice. Construction and Building Materials, vol. 438, pp. 137027, 2024.

[8] Kanavaris, F., Benedetto, G. D., Campbell, A., Gedge, G., and Kaethner, S. Reducing the embodied carbon of concrete-framed buildings through improved design and specification: Influence of building typologies, construction types and concrete mix. Structures, vol. 67, pp. 107005, 2024.

[9] Li, X., Zhou, Z., Wang, B., and Huang, W. Study on impermeability of reinforced concrete wall with horizontal construction joints. Construction and Building Materials, vol. 438, pp. 137220, 2024.

[10] Liu, Y., Qian, Z.-D., Xie, Y.-X., and Xu, S.-Q. Investigation on materials for prefabricated bridge deck pavement and construction technology: Application to a case study of concrete box-girder bridge. Case Studies in Construction Materials, vol. 20, pp. e03185, 2024.

[11] Nilimaa, J. Smart materials and technologies for sustainable concrete construction. Developments in the Built Environment, vol. 15, pp. 100177, 2023.

[12] Ren, Q., Zhang, D., Li, M., Chen, S., Tian, D., Li, H., and Liu, L. Automatic quality compliance checking in concrete dam construction:

Integrating rule syntax parsing and semantic distance. Advanced Engineering Informatics, vol. 60, pp. 102409, 2024.

[13] Shao, M., Barabash, M., Bashynska, O., Bashynskyi, Y., and Bieliatynskyi, A. Building constructions calculation models of reinforced concrete using BIM technologies. Ain Shams Engineering Journal, vol. 15(9), pp. 102894, 2024.

[14] Wu, C., Yu, Z., Shao, R., and Li, J. A comprehensive review of extraterrestrial construction, from space concrete materials to habitat structures. Engineering Structures, vol. 318, pp. 118723, 2024.

[15] Xiao, J., Liu, H., Ding, T., Yu, K., Zhang, L., Xiao, X., and Zhu, H. Rebar-free concrete construction: Concept, opportunities and challenges. Journal of Building Engineering, vol. 86, pp. 108933, 2024.

[16] Yang, M., Li, C., Liu, H., Huo, L., Yao, X., Wang, B., Yao, W., Zhang, Z., Ding, J., Zhang, Y., and Ding, X. Exploring the potential for carrying capacity and reusability of 3D printed concrete bridges: Construction, dismantlement, and reconstruction of a box arch bridge. Case Studies in Construction Materials, vol. 20, pp. e02938, 2024.

[17] Zelickman, Y., and Guest, J. K. Construction aware optimization of concrete plate thicknesses. Engineering Structures, vol. 296, pp. 116889, 2023.

[18] Zhang, S., Zhang, S., Wang, C., Zhu, G., Liu, H., and Wang, X. Extended IFC-based information exchange for construction management of roller-compacted concrete dam. Automation in Construction, vol. 163, pp. 105427, 2024.

[19] Zhang, X., Chen, K., Lu, X., Xu, G., and Chen, T. Constructional behavior of multi-span corrugated steel arch culverts stiffened by concrete rings. Journal of Constructional Steel Research, vol. 218, pp. 108751, 2024.

[20] Calvín, G., Escalero, M., Zabala, H., and Muñiz-Calvente, M. Effects of stress ratio on plasticity-induced crack closure through three-dimensional advanced numerical finite element models. Theoretical and Applied Fracture Mechanics, vol. 127, pp. 104000, 2023.

[21] Chen, J., and Zhou, X. Advanced absorbing boundaries for elastodynamic finite element analysis: The added degree of freedom method. Computer Methods in Applied Mechanics and Engineering, vol. 420, pp. 116752, 2024.

[22] Chen, Y., Zhang, J., Wang, F., and Gao, C. Hybrid substructure interacting method fusing targeted sensing data and finite element models. Engineering Structures, 314, 118314.

[23] Cheng, J., Jiang, J.-J., Xiao, R.-C., and Xiang, H.-F. Advanced aerostatic stability analysis of cable-stayed bridges using finite-element method. Computers & Structures, vol. 80(13), pp. 1145–1158, 2002.

[24] Ding, W., and Semperlotti, F. A multimesh finite element method for integral nonlocal elasticity using mesh-decoupling technique. International Journal of Mechanical Sciences, vol. 275, pp. 109260, 2024.

[25] Hauck, B., and Szekrényes, A. Advanced finite element analyses to compute the J-integral for delaminated composite plates. Applied Mathematical Modelling, 126, 584–605.

[26] Li, G., Gu, Z.-Z., Zhang, H.-Y., Ouyang, W., and Liu, S.-W. Line finite element method for geometrically nonlinear analysis of functionally graded members accounting for twisting effects. Composite Structures, vol. 343, pp. 118268, 2024.

[27] Lu, R., Li, K.-S., Wang, J., Yang, J., Zhang, X.-C., and Tu, S.-T. Understanding the small creep-fatigue crack growth mechanism of polycrystalline alloy based on crystal plasticity and extended finite element method. Engineering Fracture Mechanics, vol. 306, pp. 110172, 2024.

[28] Steinkopff, T., and Sautter, M. Simulating the elasto-plastic behavior of multiphase materials by advanced finite element techniques Part I: a rezoning technique and the multiphase element method. Computational Materials Science, vol. 4(1), pp. 10–14, 1995.

[29] Wilson, W. R. D., Schmid, S. R., and Liu, J. Advanced simulations for hot forging: Heat transfer model for use with the finite element method. Journal of Materials Processing Technology, vol. 155–156, pp. 1912–1917, 2004.

Biography

Xiao Yang graduated from Shanxi University in 2004 with a bachelor's degree in civil engineering and in 2007 with a master's degree in Taiyuan University of Technology Engineering. She is now a lecturer in the Department of Architectural Engineering, Shanxi Vocational and technical college. Her research interests include architectural acoustics, architectural structure, concrete structure and engineering mechanics.